A novel design for beamforming the Breakthrough Starshot laser array

James R. Leger
Department of Electrical and Computer Engineering
University of Minnesota, 200 Union St. SE, Minneapolis, Minnesota, USA 55455

ABSTRACT

We outline a laser array beam forming concept that is capable of meeting the laser power requirements of Breakthrough Starshot, a concept aimed at propelling spacecraft to extremely high velocities via laser radiation pressure. Our laser beam forming design offers solutions to the required laser power, optical radiance, beam steering, beam focusing, and atmospheric turbulence compensation specifications. The design consists of a large array of hexagonally close-packed optical modules. Each module contains a collimating lens illuminated by a single fiber from a coherent array of fiber amplifiers. Beam steering is accomplished by transverse micromotion of the fiber amplifier tip illuminating each collimating optic, coupled with a phase shift applied to each module by an electrooptic modulator. Overall array focus is performed by adjusting the transverse and longitudinal fiber positions of each module. Thus, by simply manipulating the position of the fiber feeds of each module and applying the appropriate phase shifts, the beam shape of the entire array can be conditioned to meet the focusing and tracking requirements of the Breakthrough Starshot concept. The same hardware can compensate for the atmospheric aberrations of piston, tilt, and quadratic curvature. For our strawman design, we calculate the overall Strehl ratio reduction of the entire array resulting from incomplete array fill factors, errors in the array phasing, finite laser bandwidth and atmospheric turbulence to be 0.36.

Keywords: Coherent laser beam addition, beam shaping, phased arrays, high power laser arrays

1. INTRODUCTION

Project Breakthough Starshot is a design study to determine whether it is possible to construct a spacecraft and propulsion system capable of reaching the local stars within a mission lifetime of approximately twenty years. To achieve this, the spacecraft would need to be accelerated to a significant fraction of the speed of light. It is easy to show that conventional rocket motors based on chemical reactions cannot achieve the required velocities. However, calculations show that radiation pressure from a suitably high radiance light source could, in principle, push on a light-weight reflecting sail with enough force to achieve speeds upwards of 20 % of the speed of light [1]. We thus envision a terrestrially mounted laser system capable of concentrating its optical power on the sail of the spacecraft a few square meters in size. The 1-2-gram spacecraft and sail would be released from a conventional satellite before being illuminated by the propulsion laser for up to 200 seconds. The laser optics would be required to track the spacecraft to compensate for the rotation of the earth during illumination, and to change focus as the spacecraft moves away from earth. An additional requirement is imposed by economics. Given the enormous size of the laser and optics, any design is likely be modular to take advantage of an economy of scale in fabrication. In addition, the optics in each module must be sufficiently simple to keep the cost low. This paper outlines a new optical design that can achieve these goals.

The specific requirements on the laser system are dependent on a number of factors. In this design study, we will assume reasonable numbers to drive the overall design. However, it is expected that the actual values will need to be adjusted as other aspects of the project are better understood. To this end, we will assume that the target star is the triple star system Alpha Centauri, with the closest star in this system, Proxima Centauri, being 4.24 light years from earth. Interest in this star has increased recently with the discovery of Proxima Centauri b, an earth-sized exoplanet thought to be orbiting in the habitable zone of Proxima Centauri.

The following requirements are assumed in the design:

- The exit aperture of the laser beam has a diameter of 2700 meters, required to achieve proper beam focusing on the spacecraft sail over the anticipated illumination period
- The total power of the laser, proposed by the flight dynamics team, is 100 GWatts
- Ytterbium-doped fiber laser amplifiers with a wavelength of 1.05 μm are chosen as the light source

- The beam must be spatially coherent across the exit aperture to achieve the required radiance
- The beam will be initially directed towards a specific target location in the sky. This location is determined by the position of the destination star at specific dates and times
- The CW laser beam must be steerable to track the target for up to 200 seconds to compensate for earth's rotation
- The system must permit beam focusing from 35.8 Megameters (geosynchronous orbit) to infinity, with closer distances desirably for other applications
- The system will be designed to compensate for atmospheric aberrations
- The system design will permit size expansion to enable higher radiance applications without excessive redesign
- The system will be fault tolerant
- The system design will be driven by cost considerations

It is anticipated that highly accurate metrology data will also be required by this system to enable the various phase compensation systems described in this paper. However, the metrology optics and the performance of the control systems are not considered in the current study. Rather we concentrate on the optical characteristics of the light generation system and describe its performance as a function of various design parameters.

2. LASER ARRAY GEOMETRY AND LAYOUT

The power-on-target specifications of most Starshot scenarios require a spatially coherent laser beam to be properly phased across an extremely large laser aperture. For instance, one scenario requires generation of a spherically phased beam directed at a target using a 2700-meter-diameter exit aperture. Conventionally, laser power is directed to a particular sky location by mounting a quasi-collimated source on a steerable gimbal so that the center of the beam is pointed in the desired direction. However, with the ultra-large apertures required by Starshot, this is clearly impractical.

An alternative design uses the layout of an optical phased array. The full aperture is divided into many sub-apertures, with each sub-aperture pointed in a fixed direction towards the target star location at zenith. This is illustrated in fig. 1, showing a side view of the array in one dimension indicating the inclination angle of each sub-aperture pointing to the target. In addition to the phase control typically found in an optical phased array, we have added control of the delivery fiber location, indicated by the x-y-z motion in the figure. We will show that this motion significantly enhances the performance of the system over a conventional phased array.

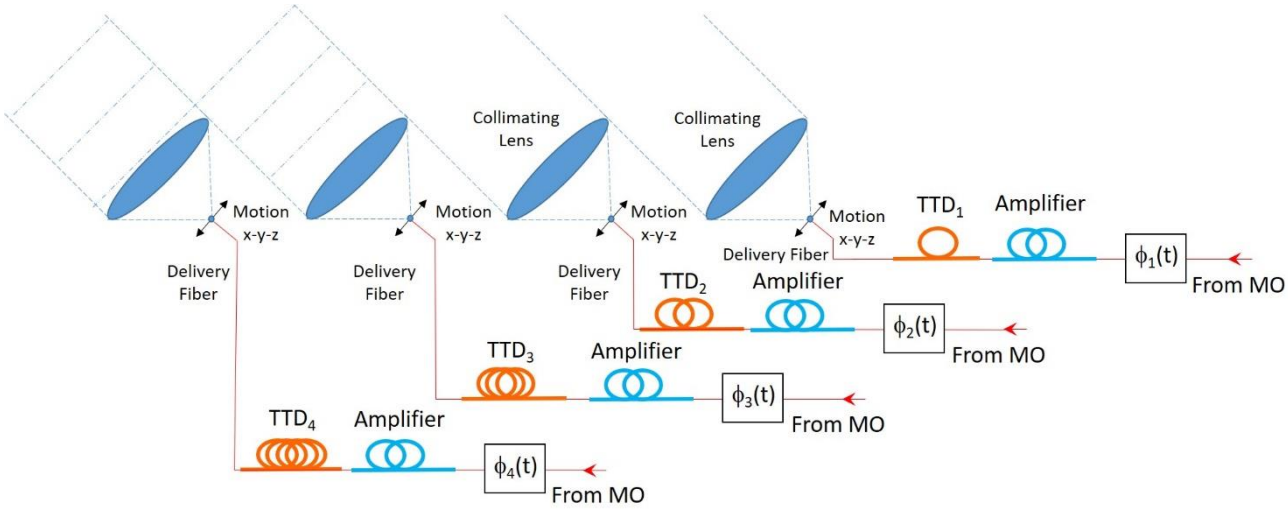

Fig. 1. Optical layout of laser array. TTD = true time delay, corresponding to additional fiber for path length balancing. MO = master oscillator. Electrooptic modulators are contained in the phase boxes.

From the perspective of the target, the overall laser array appears to be completely filled with sub-apertures, as seen in fig. 2. In this figure, each sub-aperture is illuminated by a clipped Gaussian beam from a single laser beam. The overall radiance of the combined laser beam exiting this array is reduced by three factors. First, the incomplete fill factor from the hexagonal close-packed circular sub-apertures and the nonuniform illumination of each sub-aperture produces side lobes (called grating lobes in analogy with a diffraction grating) in the far-field. Second, phase errors across the individual circular sub-apertures cause a broadening of the main lobe. Finally, (identical) phase errors across each sub-aperture produce additional side lobes. All three of these effects result in the reduction of power in the main lobe and a corresponding reduction in the amount of useful power on the spacecraft sail. The Strehl ratio can be defined as the ratio of the on-axis power in the far-field resulting from an imperfect phased array compared to the on-axis power from an equivalent full aperture filled with a perfectly uniform beam with a flat wavefront. Thus, the Strehl ratio expresses the reduction of radiance suffered by an imperfect array and can be used to estimate the reduction of performance from nonuniformities in amplitude and phase.

It can be shown [2] that the Strehl ratio S of an array is given by:

$$S = \frac{|\langle \hat{u}(r,\theta) \rangle|^2}{\langle |\hat{u}(r,\theta)|^2 \rangle} \tag{1}$$

where $\hat{u}\,(r,\theta)$ is the complex field and $\langle \cdots \rangle$ indicates a spatial average. From this equation, it is clear that the nonuniform intensity distribution shown in fig. 2 results in a reduction in the Strehl ratio of the beam. If each sub-aperture is filled by a Gaussian-shaped beam from a fiber laser, the maximum Strehl ratio that can be achieved from a hexagonally close-packed array is 0.738.

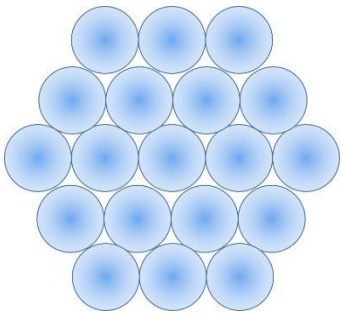

Fig. 2. View of array from perspective of target. Each sub-aperture is illuminated by a Gaussian beam.

Optical systems are available that can reshape Gaussian beams illuminating the sub-apertures into more ideal distributions [3,4], including uniformly illuminated square distributions. In this case, the full array aperture would appear to be completely uniform in amplitude and phase when viewed from the direction of light propagation, resulting in a Strehl ratio of 1.0. However, at the current time these systems involve sophisticated optical components that would increase system cost and complexity. A cost-benefit analysis would be required to determine the most beneficial approach. For the array analysis of this paper, we assume that the beams have been reshaped and that the wavefronts coming from each sub-aperture are uniform in amplitude and phase with a square shape (from the perspective of the target). The results of this analysis can then be applied to the non-beam-shaped case by multiplying the predicted radiance by the Strehl ratio reduction described above.

Returning to fig. 1, we see that each sub-aperture is fed by its own laser beam from a power amplifier, where the amplifiers share a common master oscillator. By providing the proper phase delay for each sub-aperture, the individual collimated beams can be adjusted to form a continuous plane wave across the array. In the ideal case, this resulting wavefront produces a diffraction-limited beam equivalent to an aperture that is the size of the entire array.

In the case where no beam shaping is performed, the optical components of each sub-aperture are quite simple. If the

delivery fibers from each fiber amplifier are assumed to have sufficiently large numerical apertures (> 0.15) such that no beam expansion lenses are necessary, a single collimating lens is the only optical component required for each sub-array (see fig. 1). If the delivery fibers have very low NA's, it is possible to include an expanding lens on the end of the fiber by melting a spherical cap on the fiber tip. In either case, the optical components are minimal for this part of the system.

3. BEAM STEERING AND FOCUSING

The array shown in fig. 2 consists of a large number of optical modules, where each module's sub-aperture reproduces a portion of the overall wavefront. The diameter of the sub-aperture D is chosen to match the Fried parameter described in section 6. In good seeing conditions, this can be as large as 30 cm using a wavelength of 1.05 μm. Ignoring atmospheric aberrations for the moment, we consider the diffraction properties of the full exit aperture. In the non-focusing condition, an array of uniform phase and completely filled sub-apertures produces a planar wavefront across its 2700-meter aperture. The boundary between near-field and far-field diffraction is approximately given by D^2/λ, where D is the diameter of the aperture and λ is the wavelength of light. For the proposed aperture diameter of 2700 meters and wavelength of 1.05 μm, this corresponds to a distance of 7×10^{12} meters or approximately 46 AU. For target distances that are substantially smaller than this, the beam requires positive curvature to enable the light to focus onto the target. This curvature can be applied by adjusting the phase of each sub-aperture to approximate the required spherical curvature across the array. Below we show how conditioning the wavefront of each sub-aperture by moving the fiber feed allows our proposed geometry to provide array focus as well as scan over large angles.

3.1 Array phasing requirements

The proposed phasing of the array to control target steering and focusing is shown in fig. 3. Figure 3(a) shows the beam steering component consisting of a linear phase distribution and the beam focus component consisting of a parabolic phase distribution across the entire array. The total required phase (labeled "total" in fig. 3(a)) is the sum of these two distributions. In the description below, we consider a square close-packed array for simplicity, where the integers m and n denote the $(m,n)^{\text{th}}$ sub-aperture and D is now interpreted as the spacing between sub-apertures. If we consider one particular sub-aperture located a distance mD in the x-direction and nD in the y-direction from the center of the exit aperture, we can calculate the required phase across this single sub-aperture by performing a Taylor expansion of the total phase function around points centered at the $(m,n)^{\text{th}}$ sub-aperture:

$$\phi(x,y)|_{\substack{x=mD+x' \\ y=nD+y'}} = \frac{2\pi}{\lambda}\left[\gamma_x mD - \frac{m^2D^2}{2z_0} + \gamma_y nD - \frac{n^2D^2}{2z_0}\right] + \frac{2\pi}{\lambda}\left[\gamma_x - \frac{mD}{z_0}\right]x' + \frac{2\pi}{\lambda}\left[\gamma_y - \frac{nD}{z_0}\right]y' - \frac{\pi}{\lambda z_0}[x'^2 + y'^2], \qquad (2)$$

where γ_x and γ_y are the direction cosines of beam tilt defined by $\gamma_x = cos(\theta_x)$ and $\gamma_y = cos(\theta_y)$, z_0 is the distance from the lens aperture to the geometric focal point of the focused beam, m and n are integers specifying a particular sub-aperture ranging from $\left(-\frac{M}{2}, \frac{M}{2} - 1\right)$ and $\left(-\frac{N}{2}, \frac{N}{2} - 1\right)$, M and N are the maximum number of sub-apertures in the x- and y-directions, and the coordinates (x',y') are centered in the middle of each sub-aperture.

From eq. (2) it is clear that the required phase function can be represented by four terms of the Taylor expansion. The first term is a constant and corresponds to a piston displacement of the wavefront at each sub-aperture. The second and third terms are linear functions of x' and y' and correspond to a tilt in the wavefront in the θ_x and θ_y directions. The last term is quadratic in x' and y' and corresponds to focal power.

For sufficiently narrow-band light and in an analogy with diffractive optics, we remove integer multiples of the piston term such that the overall phase shift across a sub-aperture can be minimized. Thus, eq. (2) becomes

$$\phi(x,y)|_{\substack{x=mD+x' \\ y=nD+y'}} = \frac{2\pi}{\lambda}\left[\gamma_x mD - \frac{m^2D^2}{2z_0} + \gamma_y nD - \frac{n^2D^2}{2z_0}\right]_{modulo\ 2\pi} + \frac{2\pi}{\lambda}\left[\gamma_x - \frac{mD}{z_0}\right]x' + \frac{2\pi}{\lambda}\left[\gamma_y - \frac{nD}{z_0}\right]y' - \frac{\pi}{\lambda z_0}[x'^2 + y'^2]. \qquad (3)$$

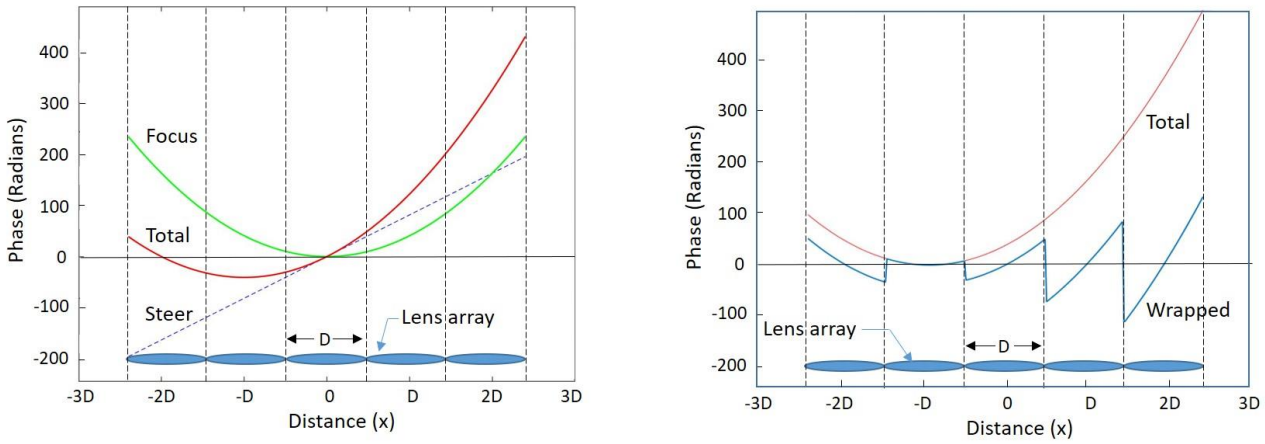

Fig. 3. Phase distribution across laser array. (a) shows the phase tilt required to steer the beam to an angle (θ_x, θ_y) *with respect to the optical axis, the parabolic curvature required to focus the beam to a point* z_0 *in front of the array, and the total required phase front; (b) shows the actual phase fronts (wrapped) applied to each sub-aperture after subtracting an integer number of wavelengths from each sub-aperture wavefront.*

Figure 3(b) shows the result of subtracting integer values of 2π from the phase of each sub-aperture. The curve labeled "wrapped" displays the phase front that is required at each sub-aperture. The modulo 2π operation preserves the proper phase relationship such that the edges of the wavefronts from adjacent sub-apertures knit together after propagation. Thus, the final wavefront labeled "total" and the wavefront labeled "wrapped" in fig. 3(b) have virtually identical optical performance.

It should be emphasized that, although there is some similarity between our proposed system and a conventional diffractive optic, there are also important differences. In a traditional diffractive lens, the entire phase function of eq. (2) is phase-wrapped modulo 2π so that the remaining phase is restricted to phase values between 0 and 2π. This allow the element to be fabricated as a surface relief structure with a maximum height of λ/(n-1), where n is the index of refraction of the substrate. The resulting diffractive lens consists of a set of rings that become progressively closer together towards the edge of the element in a manner similar to the Fresnel zones in a Fresnel Zone Plate. In our system, the phase function is divided along equal *spatial* intervals (corresponding to the spacing of the sub-apertures), and the maximum phase that must be represented across a single sub-aperture is variable and can be much greater than 2π. There is also a similarity between our system and a conventional phased array with non-steerable antennas. However, in the latter, each antenna (corresponding to a sub-aperture in our system) is a constant fixed phase. This results in a maximum scan angle θ given by $sin(\theta) = \pm\lambda/2D$. Thus, only a very small steering angle is possible using the large sub-apertures envisioned in this design. We will show below that manipulation of the launch optics in each sub-aperture permits shaping of the wavefront to match all the required terms in eq. (3), and greatly extends the utility of the design.

3.2 Shaping the sub-aperture phase distribution

The optics of the sub-apertures of fig. 1 have been redrawn in fig. 4 to show the system details, where the overall tilt of the array has been removed for simplicity. The array consists of sub-apertures spaced by *D*, each containing a lens with focal length *f* and tightly packed to achieve a 100% fill factor (*d=D,* where *d* is the illuminated area of the lens). The tip of the delivery fiber, effectively corresponding to a point source, can be moved in three directions away from the focal point of the collimating lens by an amount Δx, Δy, and Δz. It is easy to show that motion in the x'- and y'-directions can reproduce the tilt terms in eq. (3), whereas motion in the z-direction can reproduce the quadratic term. Since the piston term only needs to be applied modulo 2π, a simple phase shifter shown in fig. 1 can be used to control this final term. We note that this piston term can also be produced by an additional sub-wavelength motion in z, but we choose to implement the phase shift in this design by an electrooptic modulator.

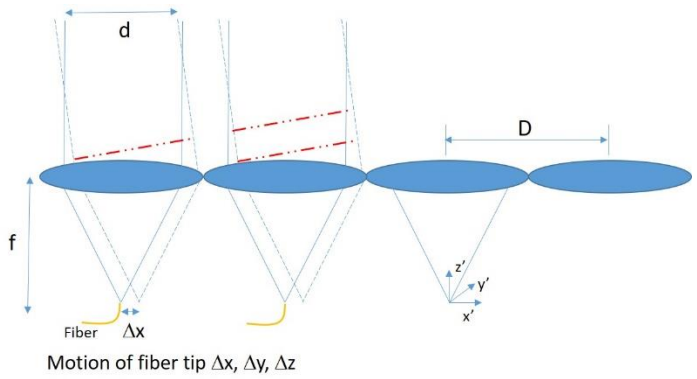

Fig. 4. Details of array with movable fiber tip. The delivery fiber can be moved in three dimensions away from the front focal point of the collimating lens.

We start by assuming that the lens system is paraxial, and that second-order optics are sufficient to model the system. This is not a requirement, and we only make this assumption to simplify the analysis. Under this approximation, the transmittance $t(x', y')$ of the collimating lens from a single sub-aperture is given by:

$$t(x', y') = \exp\left[-i\,\pi\,\frac{(x'^2+y'^2)}{\lambda f}\right], \tag{4}$$

where f is the focal length of the collimating lens. As in the previous analysis, the (x', y') coordinate system is centered on each sub-aperture (see fig. 4). Placing a point source (from the fiber tip) at the front focal point of this lens will result in a collimated beam exiting the sub-aperture.

If the point source is displaced from this front focal point by the amounts Δx, Δy, and Δz, the resulting wavefront $u(x', y')$ incident on the collimating lens is given by:

$$u(x', y') = \exp\left[i\,\pi\,\frac{(x'+\Delta x)^2+(y'+\Delta y)^2}{\lambda(f+\Delta z)}\right]. \tag{5}$$

The wavefront $u'(x', y')$ exiting the collimating lens is the product of the incident wavefront from eq. (5) and the lens transmittance from eq. (4):

$$u'(x', y') = u(x', y') \cdot t(x', y') = \exp\big(i\phi_1(x', y')\big) \cdot \exp\big(i\phi_2(x', y')\big) \cdot \exp(i\phi_3(x', y')), \tag{6}$$

where:

$$\phi_1(x', y') = \frac{\pi(x_0^2+y_0^2)}{\lambda(f+\Delta z)} \quad \text{(Piston)} \tag{7}$$

$$\phi_2(x', y') = \frac{2\pi(\Delta x x'+\Delta y y')}{\lambda(f+\Delta z)} \quad \text{(Tilt)} \tag{8}$$

$$\phi_3(x', y') = -\frac{\pi\,\Delta z\,(x'^2+y'^2)}{\lambda f(f+\Delta z)} \quad \text{(Spherical)} \tag{9}$$

It is clear that an appropriate choice of Δz in eq. (9) can reproduce the spherical component of the required wavefront in eq. (3). In particular,

$$\Delta z \cong \frac{f^2}{z_0}. \tag{10}$$

Similarly, Δx and Δy in eq. (8) can be adjusted to reproduce the tilt component in eq. (3), namely

$$\Delta x \cong f\left[\gamma_x - \frac{mD}{z_0}\right], \quad \Delta y \cong f\left[\gamma_y - \frac{nD}{z_0}\right]. \tag{11}$$

The piston component in eq. (7) can then be adjusted to reproduce the piston requirement in eq. (3). We note that, since this piston term is restricted to an excursion of 2π radians, it can easily be controlled by an electrooptic modulator. We also note that in a practical system, changes in fiber length due to thermal expansion as well as atmospheric effects are likely to dominate this system, and it is more likely that a control system will used to control this piston term to ensure that the wavefronts from adjacent sub-apertures knit together properly without any phase discontinuities. Errors introduced by this phase adjustment will reduce the Strehl ratio according to eq. (1). It is easy to show that, for small phase-only errors with a variance of σ^2, this equation reduces to

$$S = 1 - \sigma^2. \tag{12}$$

There are several current methods of performing the highly accurate motion of the fiber tip required by the above system. The most common example is the optical tracking system used in a CD and DVD player. In this system, a lens is moved transversely and longitudinally by a micro-actuator to compensate for variations in track location and disk height. The current state-of-the-art of MEMS (micro-electro-mechanical systems) technology makes mass fabrication of these mechanical translation systems practical, with the corresponding economy of scale making the actuator package highly cost effective.

4. COHERENCE REQUIREMENTS AND LASER BANDWIDTH

To achieve diffraction-limited performance from the array in fig. 1, the coherence across the array must be uniformly high. Thus, mutual coherence from the center of the array to the edge must be maintained. This implies that the path lengths of each aperture must be equalized to within the coherence time of the light from the master oscillator. For a non-focused beam with no tilt, this can be easily achieved by using additional lengths of fiber to equalize the path lengths from the master oscillator to each of the sub-apertures (see fig. 1). This path-length balancing is called establishing a "true time delay" across the elements. True time systems behave like their refractive and reflective counterparts, and can, in principle, collimate a white light source with high radiance. The bandwidth requirements of the master oscillator need only satisfy the practical variations that can be achieved by path length compensation.

When the array is used to focus and scan a beam, the piston phase term of eq. 3, which is a function of angle, focal power, and wavelength, must be considered. For a perfectly monochromatic beam, this piston term takes on a specific value that is a function of angle and focal power. However, beams with finite spectral bandwidth produce varying amounts of piston phase shift, resulting in phase discontinuities at the edges of the sub-apertures for some wavelengths and a correspondingly reduced Strehl ratio. We can calculate the necessary laser coherence length ℓ_{coh} and bandwidth $\Delta\nu_{max}$ for a specific propagation angle (γ_x, γ_y) and focal distance z_0 by simply requiring the maximum change in optical path length of this piston term to be less than $\bar{\lambda}/4$, where $\bar{\lambda}$ is the average wavelength:

$$\Delta\nu_{max} = c/(\ell_{coh})$$
$$\text{where } \ell_{coh} = 4\left\{\left[\gamma_x mD - \frac{m^2D^2}{2z_0} + \gamma_y nD - \frac{n^2D^2}{2z_0}\right]_{max} - \left[\gamma_x mD - \frac{m^2D^2}{2z_0} + \gamma_y nD - \frac{n^2D^2}{2z_0}\right]_{min}\right\} \tag{13}$$

and the maxima and minima are computed with respect to the sub-aperture indices *m* and *n*. If the master oscillator contains frequencies that are uniformly distributed from $-\Delta\nu_{max}/2$ to $-\Delta\nu_{max}/2$, this phase error reduces the Strehl ratio by a factor of 0.8.

5. COMPENSATION FOR THERMAL DRIFT IN FIBERS AND FREE-SPACE OPTICS

Returning to figure 1(a), we see that the same micro-positioner element that is used to steer and focus the beam can be used to compensate for any positional changes in the free-space optics. This position alignment is very critical to the wavefront shape and will need to be compensated by an interferometric feedback loop. Control in the transverse direction can compensate for linear phase distortions detected in the collimated beam from each sub-aperture. Correspondingly, quadratic phase errors that result from expansion in the stage that separates the fiber from the lens can be compensated by motion of the fiber tip in the longitudinal (or optical axis) position. Each of these controls can be guided by interferometric measurements of the wavefront.

The piston errors of the fiber feed come from thermally induced expansion of the amplifier fibers and changes in ambient temperature in the delivery fibers. With a proper feedback signal from an interferometric measurement system, this can be compensated by the electrooptic phase shifter shown in fig. 1. Typical phase shifts when the fiber is first turned on can be thousands of waves, even for a short fiber, and it may be impractical to assume that a phase modulator can track and cancel this large of a phase excursion. However, we recall that the piston term only needs to be corrected to modulo 2π radians in phase. The additional phase discrepancy may require a system with narrow bandwidth to ensure coherence, but it can, in principle, be corrected by a simple modulator with a zero-to-2π phase modulator. This phase condition is of critical importance in achieving diffraction-limited performance, as the piston error must be kept uniformly low across the entire array.

6. COMPENSATION FOR ATMOSPHERIC TURBULENCE

We now consider the practical effects of propagating laser light through the atmosphere. A coarse estimate of the effect of the atmosphere on the Strehl ratio is given by the Fried parameter r_0, which is the diameter over which the atmosphere can be considered approximately uniform in phase. The phase error σ_ϕ^2 observed over an aperture of size D is then given by

$$\sigma_\phi^2 = K \left(\frac{D}{r_0}\right)^{5/3} \text{ rad}^2 \tag{14}$$

where K = 1.26 when the piston error only is corrected and K = 0.18 when both piston and tip/tilt are corrected. We note that our system is, in principle, capable of canceling aberrations out to the second order (i.e. quadratic). However, measuring this aberration is more difficult and we choose to only implement the piston and tip/tilt correction.

To calculate the maximum aperture that can be used, we need to know the Fried parameter and the wavelength. Good seeing results in Fried parameters on the order of 10 cm at a wavelength of 500 nm. The Fried parameter is known to scale with wavelength according to $\lambda^{6/5}$. Consequently, the Fried parameter at 1.05 micrometer radiation corresponding to the same good seeing is expected to be on the order of 25 cm. This leads to the choice of 30 cm sub-aperture diameters for our straw man system. With proper metrology, the control systems described in this paper should be able to compensate for atmospheric turbulence across 30 cm apertures.

The effect of atmospheric turbulence on the Strehl ratio can be calculated by combining eq. (14) with eq. (12), resulting in

$$S = 1 - K \left(\frac{D}{r_0}\right)^{5/3}, \tag{15}$$

where we have assumed that the phase error is small. For the case where $D = 30\ cm$, $r_0 = 25\ cm$, and K = 0.18 (i.e. piston and tip/tilt correction), the Strehl ratio is given by $S = 0.76$.

7. FAULT TOLERANCE CONSIDERATIONS

The proposed system is highly modular, and hence is inherently fault tolerant. Failure of individual modules will not prevent the entire system from functioning. However, it should be noted that a coherent array is reduced by the square of the number of array elements lost. This is because the total on-axis power is reduced by two factors: i) the overall power

of the array is reduced by the ratio of the number of functioning modules to the initial number in the array; ii) the fill factor of the array is reduced by this same number. Eq. (1) indicates that the Strehl ratio is proportional to the fill factor, reducing the amount of on-axis power by this same amount. Hence, the total amount of on-axis power is reduced by

$$P_{on-axis} = P_0 \cdot \frac{M_{active}}{M_{initial}} \cdot (fill\ factor\ reduction) = P_0 \cdot \left(\frac{M_{active}}{M_{initial}}\right)^2 \quad (16)$$

where $P_{on-axis}$ is the on-axis power applied to the target, P_0 is the on-axis power from the fully functioning array, M_{active} is the number of modules that are functioning in the array, and $M_{initial}$ is the planned number of modules in a fully functioning array.

8. PERFORMANCE CALCULATIONS

In this section, we assume several parameters and calculate the performance of the system.

Assumptions:

- Geographic location of array: Atacama Desert, Chile
- Height of Alpha Centauri at zenith: 51 degrees
- Laser wavelength: 1.05 μm
- Gaussian beam illumination with hexagonally close packed circular apertures
- Fried parameter: 10 cm at 500 nm wavelength (25 cm at operating wavelength)
- Focal length of collimating lenses: 1 meter
- Array shape and size: circular; 2700 meter diameter
- Tracking time: 200 seconds
- Maximum steering angle required for tracking: 19.1 mrad.
- Target distance at closest approach: $z_0 = 35.8$ Megameters (geosynchronous orbit)

Estimated operating parameters:

- Number of sub-apertures across diameter (N) = 9000
- Diameter of beam sub-aperture: 30 cm
- Total number of hexagonally close-packed sub-apertures (M) = $\frac{Area_{array}}{Area_{sub-aperture}} \times 0.907 = 73{,}467{,}000$
- Atmospheric turbulence correction of piston and tilt: Strehl ratio: 0.76
- Maximum transverse fiber movement required for tracking: 19.1 mm
- Maximum transverse fiber movement required for focus at geosynchronous orbit: 38 μm
- Maximum longitudinal fiber movement required for focus at geosynchronous orbit: 28 nm (i.e. not necessary to perform this movement for target at this distance)
- Transverse fiber movement tolerance: $\ll 3.5$ μm
- Estimated Strehl ratio due to Gaussian illuminated sub-apertures in a hexagonally close-packed array, atmospheric turbulence with Fried parameter of 10 cm (λ = 500 nm), a bandwidth of 2.9 MHz, and phase error of feedback system (P-V = π/2 radians): (0.74) (0.76) (0.8) (0.8) = 0.36
- Total power per aperture required to concentrate 100 GWatts on target: 3.7 Kilowatts
- Required coherence length: 103 meters (for $\gamma_x = \pm\frac{19.1}{2}$ milliradians)
- Required laser bandwidth (based on coherence length requirement for beam steering): < 2.9 MHz (for $\gamma_x = \pm\frac{19.1}{2}$ milliradians)

9. CONCLUSIONS

We have outlined a design of a large laser array capable of meeting the performance requirements of the Breakthrough Starshot laser source. These requirements include overall source radiance, beam steering, beam focusing, and atmospheric aberration compensation. Our design contains no large moving parts and can, in principle, be implemented with low-cost components. We have evaluated the overall Strehl ratio of the system to estimate the power losses of the system. Our final design requires a single laser amplifier module to produce approximately 3.7 KWatts of single-spatial mode optical

power with a bandwidth of less than 3 MHz. We note that there are still many parts of the laser system that have not been addressed in this analysis, including the metrology and control systems that would be required for successful implementation. Assuming that these problems can be solved, the proposed architecture appears to be able to achieve the basic laser requirements for radiation pressure-driven spacecraft propulsion.

References

[1] Parkin, Kevin L.G., "Breakthrough Starshot system model," *Acta Astronautica* **152** (2018), 370-384 (2018)

[2] J. R. Leger, "External Methods of Phase Locking and Coherent Beam Addition," Chapter 8 of the book *Surface Emitting Semiconductor Lasers and Arrays*, G. Evans and J. Hammer, ed., Academic Press, New York (1993).

[3] Mendlovic, David and Ozaktas, Haldum M., "Optical-coordinate transformation methods and optical-interconnection architectures," *Appl. Opt.* **32**, 5119 (1993).

[4] Dickey, F.M. and Holswade, S.C., "Laser Beam Shaping-Theory and Techniques", Marcel Dekker, Inc. (2000).

Acknowledgments

This project was funded through a contract from the University of Southampton as part of the Breakthrough Initiatives, a division of the Breakthrough Prize Foundation. We are grateful for their support and technical collaboration.